Advanced Distributed Wind Turbine Controls Series: Part 1–Flatirons Campus Model Overview

Microgrids, Infrastructure Resilience, and Advanced Controls Launchpad (MIRACL)

Benjamin Anderson, Ram Poudel, Jim Reilly, Przemyslaw Koralewicz, Venkat Krishnan, and Jayaraj Rane

National Renewable Energy Laboratory

NREL is a national laboratory of the U.S. Department of Energy
Office of Energy Efficiency & Renewable Energy
Operated by the Alliance for Sustainable Energy, LLC

This report is available at no cost from the National Renewable Energy Laboratory (NREL) at www.nrel.gov/publications.

Contract No. DE-AC36-08GO28308

Technical Report
NREL/TP-5000-81338
July 2022

Advanced Distributed Wind Turbine Controls Series: Part 1–Flatirons Campus Model Overview

Microgrids, Infrastructure Resilience, and Advanced Controls Launchpad (MIRACL)

Benjamin Anderson, Ram Poudel, Jim Reilly, Przemyslaw Koralewicz, Venkat Krishnan, and Jayaraj Rane

National Renewable Energy Laboratory

Suggested Citation
Anderson, Benjamin, Ram Poudel, Jim Reilly, Przemyslaw Koralewicz, Venkat Krishnan, and Jayaraj Rane. 2022. *Advanced Distributed Wind Turbine Controls Series: Part 1–Flatirons Campus Model Overview; Microgrids, Infrastructure Resilience, and Advanced Controls Launchpad (MIRACL)*. Golden, CO: National Renewable Energy Laboratory. NREL/TP-5000-81338. https://www.nrel.gov/docs/fy22osti/81338.pdf.

NREL is a national laboratory of the U.S. Department of Energy
Office of Energy Efficiency & Renewable Energy
Operated by the Alliance for Sustainable Energy, LLC

This report is available at no cost from the National Renewable Energy Laboratory (NREL) at www.nrel.gov/publications.

Contract No. DE-AC36-08GO28308

Technical Report
NREL/TP-5000-81338
July 2022

National Renewable Energy Laboratory
15013 Denver West Parkway
Golden, CO 80401
303-275-3000 • www.nrel.gov

NOTICE

This work was authored by the National Renewable Energy Laboratory, operated by Alliance for Sustainable Energy, LLC, for the U.S. Department of Energy (DOE) under Contract No. DE-AC36-08GO28308. Funding provided by the U.S. Department of Energy Office of Energy Efficiency and Renewable Energy Wind Energy Technologies Office. The views expressed herein do not necessarily represent the views of the DOE or the U.S. Government.

This report is available at no cost from the National Renewable Energy Laboratory (NREL) at www.nrel.gov/publications.

U.S. Department of Energy (DOE) reports produced after 1991 and a growing number of pre-1991 documents are available free via www.OSTI.gov.

Cover Photos by Dennis Schroeder: (clockwise, left to right) NREL 51934, NREL 45897, NREL 42160, NREL 45891, NREL 48097, NREL 46526.

NREL prints on paper that contains recycled content.

Acknowledgments

We are thankful to all project team members from partnering laboratories on the Microgrids, Infrastructure Resilience, and Advanced Controls Launchpad (MIRACL) project:

- Idaho National Laboratory
- Pacific Northwest National Laboratory
- Sandia National Laboratories.

We also express our sincere gratitude to our industry advisory board members for their valuable insights and real-world test system recommendations during the March 2020 advisory board meeting: Venkat Banunarayanan (National Rural Electric Cooperative Association), Chris Rose (Renewable Energy Alaska), Rob Wills (Intergrid), Paul Dockrill (Natural Resource Canada), Jeff Pack (POWER Engineers), Arvind Tiwari (GE Global Research), Kristin Swenson (Midcontinent Independent System Operator), Jonathon Monken (PJM), and Scott Fouts (QED Wind Power).

In addition, we would like to thank Brian Naughton, Rachid Darbali-Zamora, and Ricardo Castillo for their thoughtful peer reviews, and Sheri Anstedt and Amy Brice for editorial support.

This report is available at no cost from the National Renewable Energy Laboratory (NREL) at www.nrel.gov/publications.

List of Abbreviations and Acronyms

BESS	battery energy storage system
CART	Controls Advanced Research Turbine
DERs	distributed energy resources
FRT	fault ride-through
IEEE	Institute of Electrical and Electronics Engineers
kHz	kilohertz
kV	kilovolt
kVA	kilovolt-ampere
kW	kilowatt
m/s	meters per second
ms	millisecond
µs	microsecond
MIRACL	Microgrids, Infrastructure Resilience, and Advanced Controls Launchpad
MVA	megavolt-ampere
NREL	National Renewable Energy Laboratory
pu	per unit of the baseline value
PV	photovoltaics
s	second
V	volt
VAC	volts alternating current
VDC	volts direct current
W	watt
µs	microsecond

This report is available at no cost from the National Renewable Energy Laboratory (NREL) at www.nrel.gov/publications.

Executive Summary

In addition to generating energy for the power system that they are connected to, wind turbines—through their rotating masses and inverter-based controls—can enable various reliability and resilience services using advanced controls. As part of the Microgrids, Infrastructure Resilience, and Advanced Controls Launchpad (MIRACL), we demonstrate that advanced wind turbine controls can be employed to support higher contributions of wind energy, and that wind turbines can support grid stability in islanded or grid-connected configurations. This report documents models of various subsystems within the National Renewable Energy Laboratory's Flatirons Campus that will be used in three subsequent reports to demonstrate capabilities of advanced wind turbine controls. The series of reports will detail the advanced capabilities of distributed wind turbines to provide support to isolated grids, distribution grids, and microgrids.

We develop models to simulate a 600-kilowatt wind turbine, 430-kilowatt solar photovoltaic array, 1-megawatt/1-megawatt-hour battery energy storage system, 2-megawatt diesel generator, and critical and dynamic loads. The models of the subsystems in MATLAB Simulink are validated with data from real-world components on the Flatirons Campus. These validated models can be configured for various studies, including four MIRACL use cases: (1) isolated grids, (2) microgrids, (3) behind-the-meter wind turbine deployments, and (4) front-of-the-meter wind turbine deployments.

This report is available at no cost from the National Renewable Energy Laboratory (NREL) at www.nrel.gov/publications.

Table of Contents

This report is available at no cost from the National Renewable Energy Laboratory (NREL) at www.nrel.gov/publications.

List of Figures

List of Tables

This report is available at no cost from the National Renewable Energy Laboratory (NREL) at www.nrel.gov/publications.

1 Introduction

Distributed renewable energy resources can provide both resilience and economic benefits. As a growing portion of renewable energy generation sources are integrated into power systems, their ability to provide essential grid services beyond energy becomes increasingly important. Advanced control methodologies can enable distributed wind turbines to provide grid services and thus play an enhanced role in the generation mix.

The research road map of distributed wind controls (Reilly, Poudel, et al. 2021) for the Microgrids, Infrastructure Resilience, and Advanced Controls Launchpad (MIRACL) documents a literature review of active and reactive control capabilities of different distributed energy resources (DERs) and develops a road map for the application of such control technologies for distributed wind turbines. The road map envisions developing advanced controls for distributed wind turbines in four use cases, as defined by the multilaboratory MIRACL team (Reilly, Gentle, et al. 2021): (1) isolated grids, (2) microgrids, (3) behind-the-meter wind turbine deployments, and (4) front-of-the-meter wind turbine deployments.

This report provides details for MATLAB Simulink models developed to simulate the Controls Advanced Research Turbine (CART) and various assets at the National Renewable Energy Laboratory's (NREL's) Flatirons Campus. The models were configured to represent the four MIRACL use cases to increase understanding of the enhanced role of distributed wind energy in the evolving grid. The results from applying the models to the use case configurations will be published as a series of reports with the following titles:

- Advanced Distributed Wind Turbine Controls Series: Part 1—Flatirons Campus Model Overview
- Advanced Distributed Wind Turbine Controls Series: Part 2—Wind Energy in Isolated Grids
- Advanced Distributed Wind Turbine Controls Series: Part 3—Wind Energy in Grid-Connected Deployments
- Advanced Distributed Wind Turbine Controls Series: Part 4—Wind Energy in Microgrids.

The models will be made publicly available to provide access to industry and academia. In future work, the model will be validated through hardware-in-the-loop simulation at the Flatirons Campus.

This report is available at no cost from the National Renewable Energy Laboratory (NREL) at www.nrel.gov/publications.

2 Flatirons Campus Model

This section presents a Flatirons Campus model overview, configurations, and component descriptions. The model can be found on GitHub (Anderson 2021).

2.1 Flatirons Campus Model Overview

The MIRACL team chose a small portion of NREL's Flatirons Campus that could be configured—in both a physical and a simulated environment—to represent the four MIRACL distributed wind use cases. The Flatirons Campus normally operates in grid-connected mode but was configured in 2020 to also operate in an islanded/isolated mode, as needed. The Flatirons Campus grid has two 13.2-kilovolt (kV) line-line buses: regular grid (utility grid bus) and controllable grid interface (CGI bus). Figure 1 portrays the Flatirons Campus grid infrastructure along with the connections to the two buses.

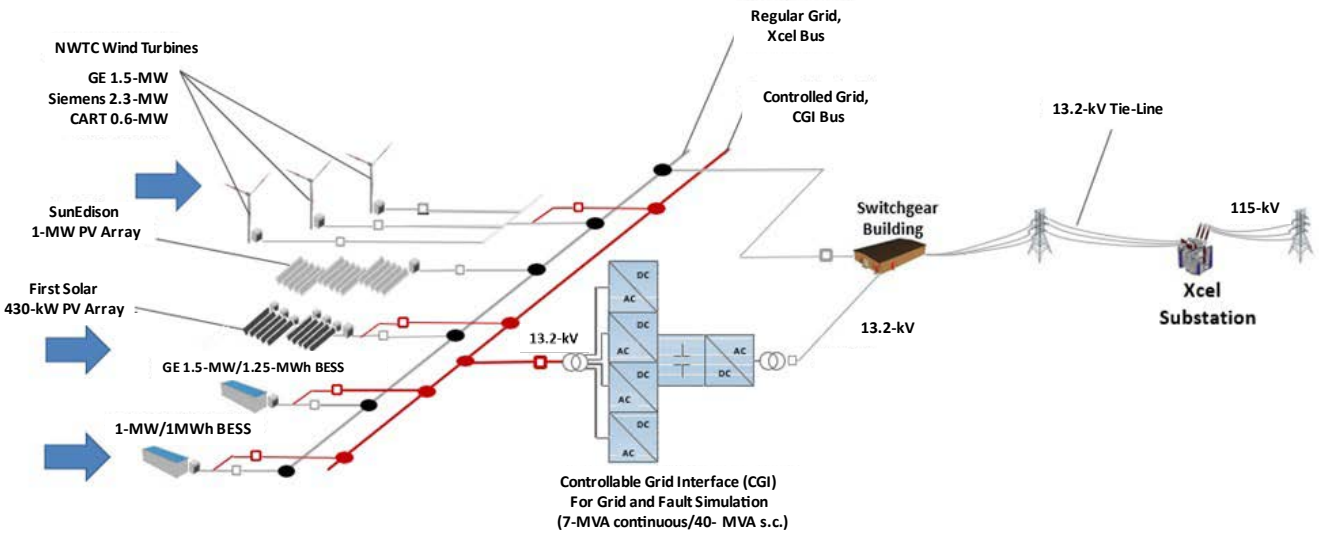

Figure 1. Flatirons Campus grid configuration/infrastructure.

BESS = battery energy storage system; CART = Controls Advanced Research Turbine; GE = General Electric; NWTC = National Wind Technology Center; PV = photovoltaics; s.c. = short circuit.

The following assets were chosen for the Flatirons Campus model. All are connected via transformers to the 13.2-kV medium-voltage bus:

- Distributed wind: three-bladed CART 600-kilowatt (kW) wind turbine
- Solar photovoltaics (PV): First Solar 430-kW PV plant and SunEdison 1-megawatt (MW) PV plant

This report is available at no cost from the National Renewable Energy Laboratory (NREL) at www.nrel.gov/publications.

- Storage: 1-MW/1-megawatt-hour (MWh) RES Americas battery energy storage system (BESS)
- Critical and deferrable loads
- Controllable grid interface: 7-megavolt-ampere (MVA) back-to-back converter system to simulate grid faults without impacting the utility grid.
- 2-MW diesel generator (used temporarily during islanded operation)

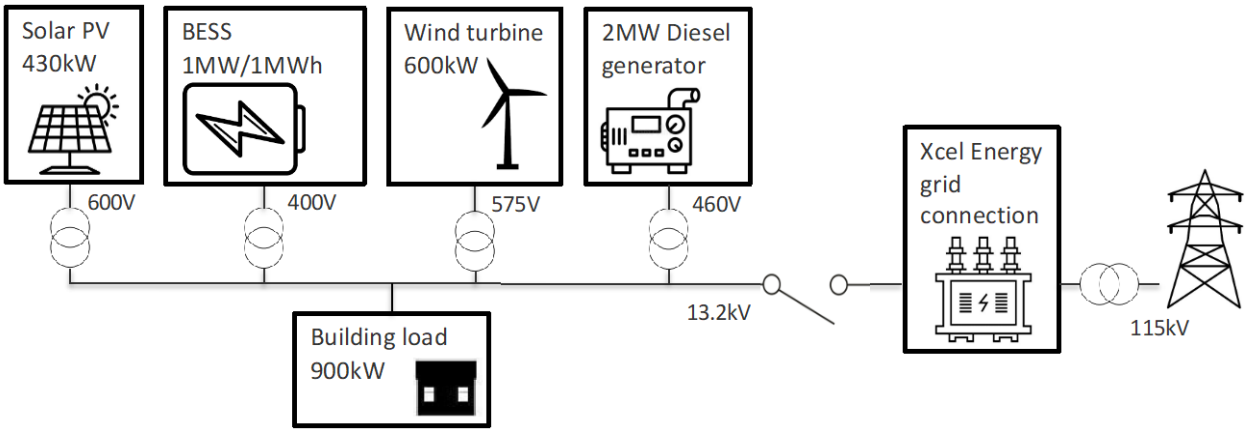

Figure 2. One-line diagram of the Flatirons Campus microgrid under study

Figure 2 presents a diagram of the microgrid used in this study (with a snapshot of load composition and fault location). More detailed information about the Flatirons Campus grid and both past and ongoing work can be found at (NREL n.d.). Many of the components at the Flatirons Campus are for research purposes and are not used as power generation sources under normal operating conditions. The distributed generation assets at the Flatirons Campus can be managed using a hybrid plant controller that routes energy generated from wind turbines and solar PV directly to loads while managing deficits and surplus with storage devices such as battery banks or through curtailment of the generation sources.

2.2 Flatirons Campus Model Configuration

The MATLAB Simulink model can be configured for the four use cases defined by the multilaboratory MIRACL team (Reilly, Gentle, et al. 2021): (1) isolated grids, (2) microgrids, (3) behind-the-meter wind turbine deployments, and (4) front-of-the-meter wind turbine deployments. The switch in Figure 3 is the isolation device between the Flatirons Campus and the utility grid. With the breaker closed, the model represents a grid-connected system (either in front of or behind the meter) and microgrid in grid-connected mode. With the breaker open, the model represents an isolated grid and a microgrid in island mode. By opening or closing the breaker, microgrid transitions between island mode and grid-connected mode are studied.

This report is available at no cost from the National Renewable Energy Laboratory (NREL) at www.nrel.gov/publications.

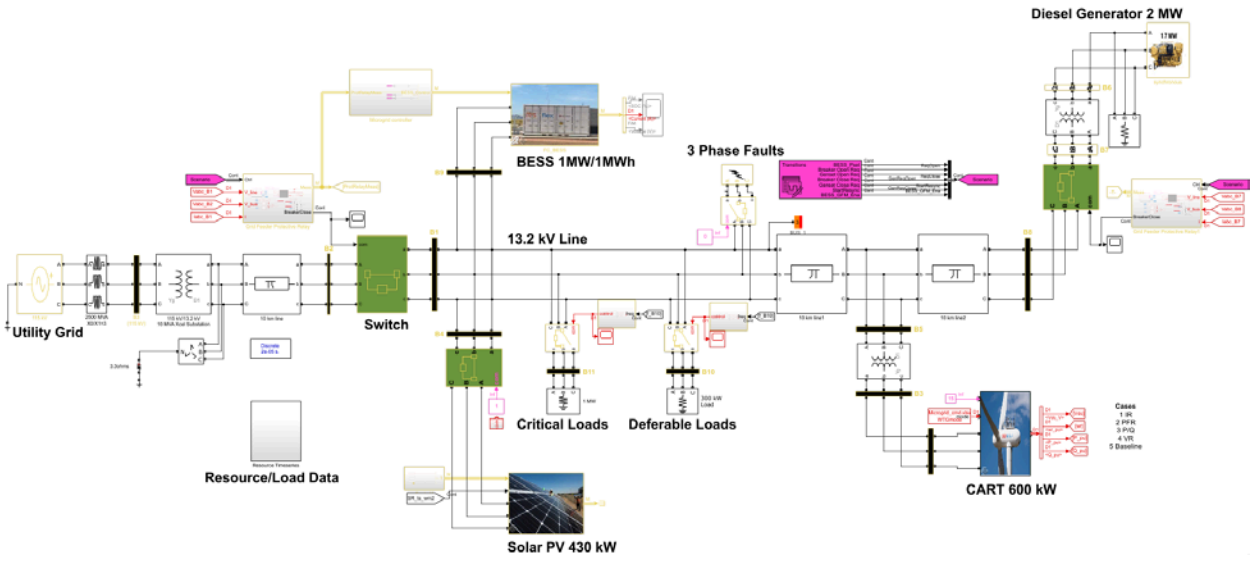

Figure 3. Flatirons Campus MATLAB Simulink model. (Details can be found in the Simulink model on GitHub [Anderson 2021]).

2.3 Flatirons Campus Model Fidelity

Averaged models represent power electronic devices that use equivalent voltage sources to generate the AC voltage averaged over one cycle of the switching frequency. A similar method is used for DC-DC converters. An averaged model does not resolve harmonics, but the relatively slower electromagnetic and electromechanical dynamics resulting from control system and power system disturbances are preserved.

In this case, given the focus on developing controls and studying the use of grid-forming inverters for black start (providing inrush current and voltage and frequency stability), we developed an averaged model of the Flatirons Campus and supported it with higher-fidelity models as needed (Poudel et al. 2021). The model uses a discrete time step of 50 microseconds (μs). Given the focus on 1- to 50-s post-fault responses, the averaged model is the best option to quantify the reliability benefits from advanced distributed wind turbine controls. For future work that focuses on using larger time scales, such as dispatch over a longer time horizon, mitigating variability and uncertainty, ramping over multiple days, and quantifying economic value and market prices, we will consider using lower-fidelity performance or phasor models of the microgrid.

2.4 Flatirons Campus Model Components

2.4.1 Wind Turbine: Averaged Model

Averaged models represent power electronic devices that use equivalent voltage sources to generate the AC voltage averaged over one cycle of the switching frequency. A similar method is used for DC-DC converters. The averaged model does not resolve harmonics, but the relatively slower electromagnetic and electromechanical dynamics resulting from control system and power system disturbances are preserved. We have used an averaged model of the wind turbine with a discrete time step of 50 μs.

This report is available at no cost from the National Renewable Energy Laboratory (NREL) at www.nrel.gov/publications.

The CART at the Flatirons Campus is a 600-kW turbine with a customized and reprogrammable real-time controller specially designed to study advanced control concepts (Fingersh and Johnson 2002). A detailed specification of the CART is provided in (Ashuri et al. 2016). The CART employs the Type IV (full converter) configuration (Wang et al. 2018) along with an ABB drive. We developed an averaged model of the CART in MATLAB Simulink by adapting a stock Simulink Type IV wind turbine averaged model (Gagnon and Brochu 2020), as shown in Figure 4. The model includes a customizable wind turbine, drivetrain, generator, and converters. We changed the turbine rating to 600 kW at 11.7 meters per second (m/s), replaced the stock power coefficient curve with a power coefficient lookup table characterizing the CART, updated the drivetrain inertia and stiffness, and added a variety of control functionalities, as detailed in Section 3.

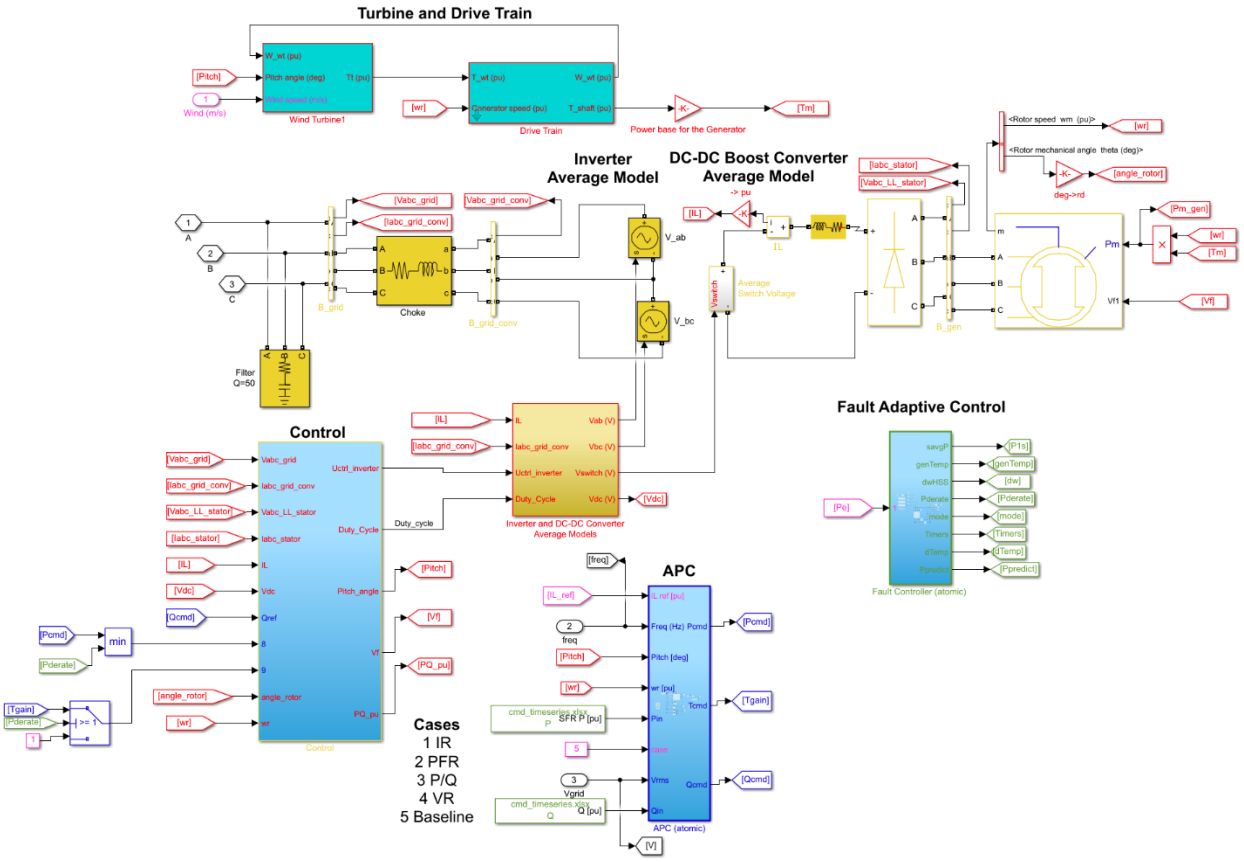

Figure 4. CART averaged Simulink model.

IR = inertial response; PFR = primary frequency response; P/Q = real/reactive power; VR = voltage response.

We integrated grid-side inverter controls from a separate hybrid wind turbine model developed by (Trevisan et al. 2018) into the CART model. The hybrid model provides an accuracy near that of a detailed model but with the computational time of an averaged model. This reduces the CART model's response time to reactive power commands and improves its voltage fault ride-through capabilities, as the hybrid model has a fast, non-oscillatory reactive power control. A more detailed explanation of the hybrid model is available in the Appendix.

This report is available at no cost from the National Renewable Energy Laboratory (NREL) at www.nrel.gov/publications.

2.4.2 Grid-Forming Inverter

Inverters can be grid-following or grid-forming. An inverter evaluates power flow parameters and commands a power reference to a generator. The reference power command helps bring the power system AC parameters, such as voltage and frequency, to desired levels. Along with the grid-forming diesel generator, the grid-forming inverter can black start the system in case of an outage.

In this study, a grid-forming inverter, connected to the BESS, is modeled to reflect the working of the SMA inverter at the Flatirons Campus grid. (The same inverter model, in grid-following mode, is connected to the PV model). The model works by generating a three-phase voltage source corresponding to the state of the power system. The inverter in grid-forming mode uses the voltage and frequency as the set points to generate the three-phase voltage source. The following two equations based on frequency (f) and voltage (V) are used to calculate reference active power P_{ref} and reactive power Q_{ref}:

$$f = f_{\text{ref}} + k^P \times (P_{\text{ref}} - P_{\text{measured}}) \quad (1)$$

$$V = V_{\text{ref}} + k^V \times (Q_{\text{ref}} - Q_{\text{measured}}) \quad (2)$$

where k^P and k^V are corresponding droop parameters.

Figure 5 presents the model of the inverter used in this study. This inverter has the capability to operate in either grid-following or grid-forming mode. The inverter receives various control set points (e.g., P_{ref} and Q_{ref} in grid-following mode, and V_{ref} and f_{ref} in grid-forming mode) and outputs the reference U_{abc_ref} for the inverter.

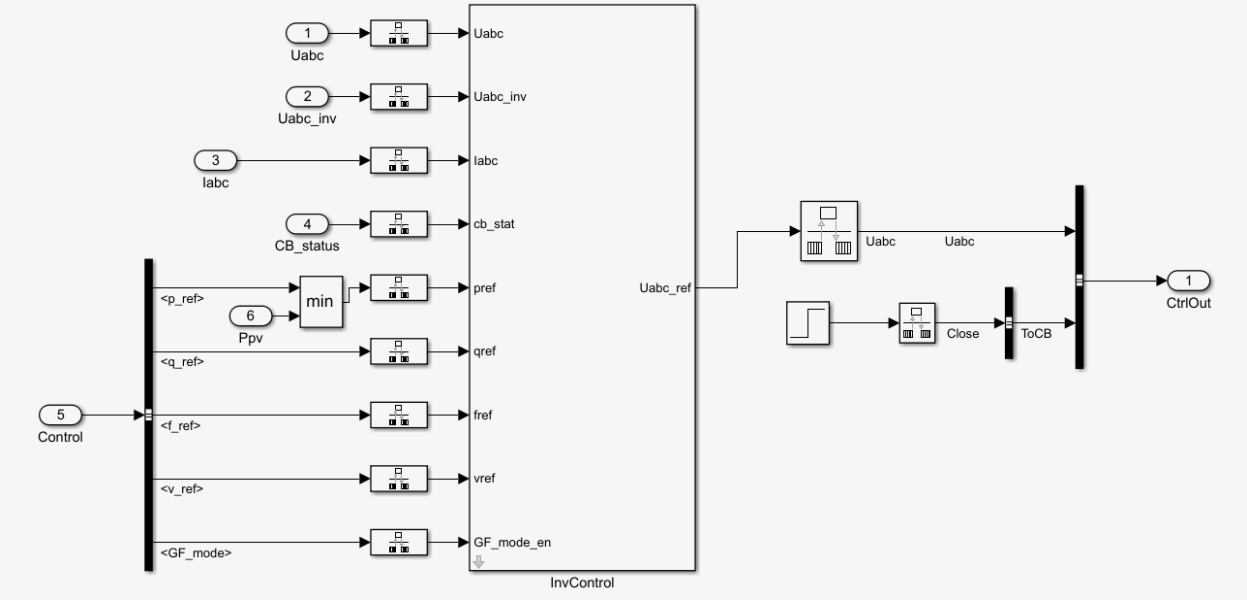

Figure 5. Simulink model of the inverter

This report is available at no cost from the National Renewable Energy Laboratory (NREL) at www.nrel.gov/publications.

2.4.3 Solar Photovoltaics

The 430-kW First Solar PV plant at the Flatirons Campus is modeled. This solar PV plant uses a First Solar Series 4 105-watt (W) module to convert the solar irradiance into electric power. The plant employs six string inverters, two 125-kW inverters (1,500 volts direct current [VDC] to 600 volts alternating current [VAC]) and four 45-kW inverters (1,500 VDC to 600 VAC). First Solar's power plant controller system maintains its integration with the utility grid's 13.2-kV AC bus. Figure 6 presents the arrangement of various components of the PV plant as represented in the Simulink model. It comprises a 500-kilvolt-ampere (kVA), 600-V/13.2-kV transformer, 430-kW PV array and a maximum power point tracking controller that uses a perturb-and-observe technique (MathWorks 2020) in the range of 0 V to approximately 1,500 V. The inverter can operate in both grid-following and grid-forming modes.

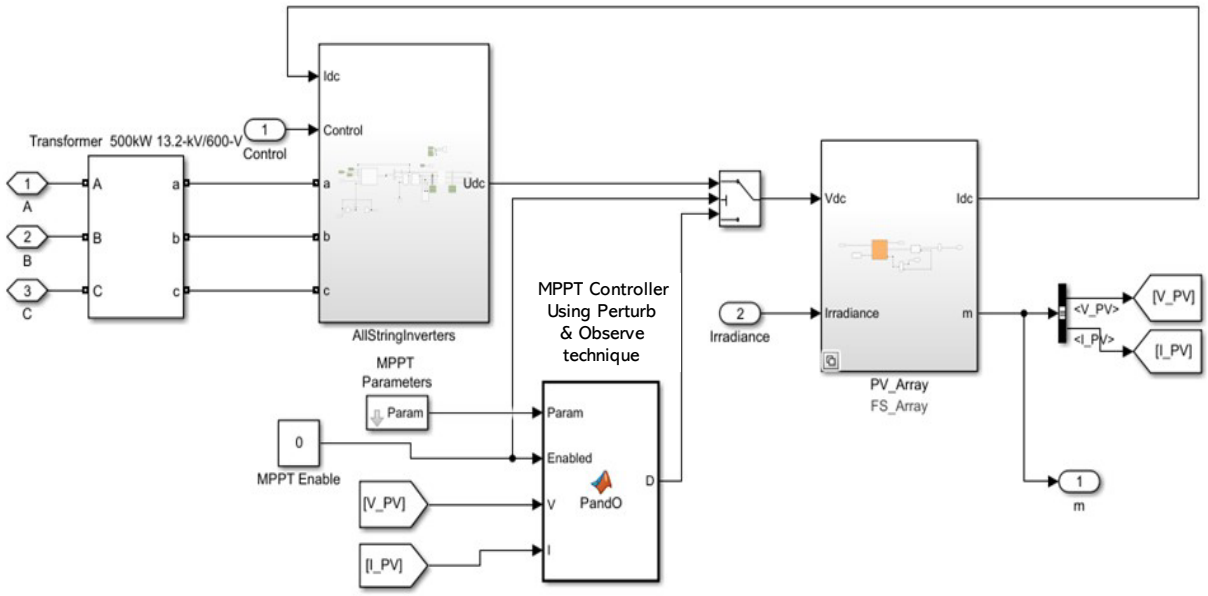

Figure 6. First Solar PV array Simulink model.

MPPT = maximum power point tracking.

2.4.4 Battery Energy Storage System

The RES Americas 1-MW/1-MWh BESS at the Flatirons Campus is modeled. The BESS is used to conduct testing and demonstration of several types of grid support services. A detailed technical specification is documented in (Kuga et al. 2019). The BESS system comprises a 2.3-MVA inverter from SMA, a 0.4-kV | 13.2-kV (1-MVA) transformer, and Eaton switchgear, among other balance-of-systems components. Figure 7 provides the MATLAB Simulink model of the BESS, with grid-following (current source) and grid-forming (voltage source) functionalities. The BESS has an inverter, so it is AC-coupled with the other devices in the microgrid. The configuration of an AC-coupled BESS with a wind turbine and solar PV could supply the islanded Flatirons Campus grid during an emergency event and maintain grid frequency and voltage stability.

This report is available at no cost from the National Renewable Energy Laboratory (NREL) at www.nrel.gov/publications.

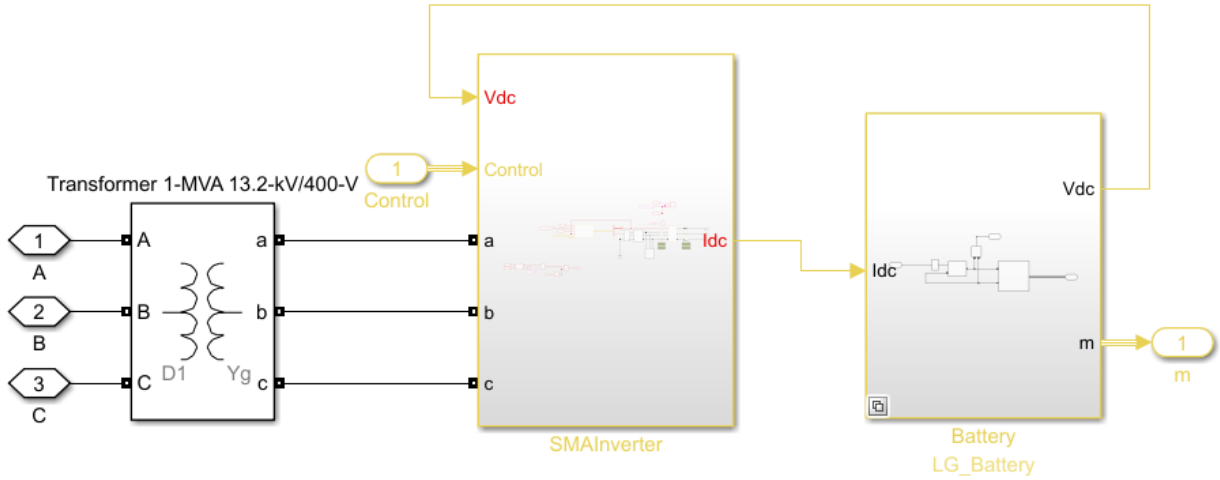

Figure 7. BESS Simulink model

We have also simulated an integrated BESS in the DC link of the wind turbine. The DC-coupled BESS system utilizes the grid-side converter for normal operation of the microgrid. For the wind turbine to support black start, the grid-side converter can be replaced by a grid-forming inverter. Figure 8 presents the layout of the DC-coupled BESS in the DC-link of the wind turbine.

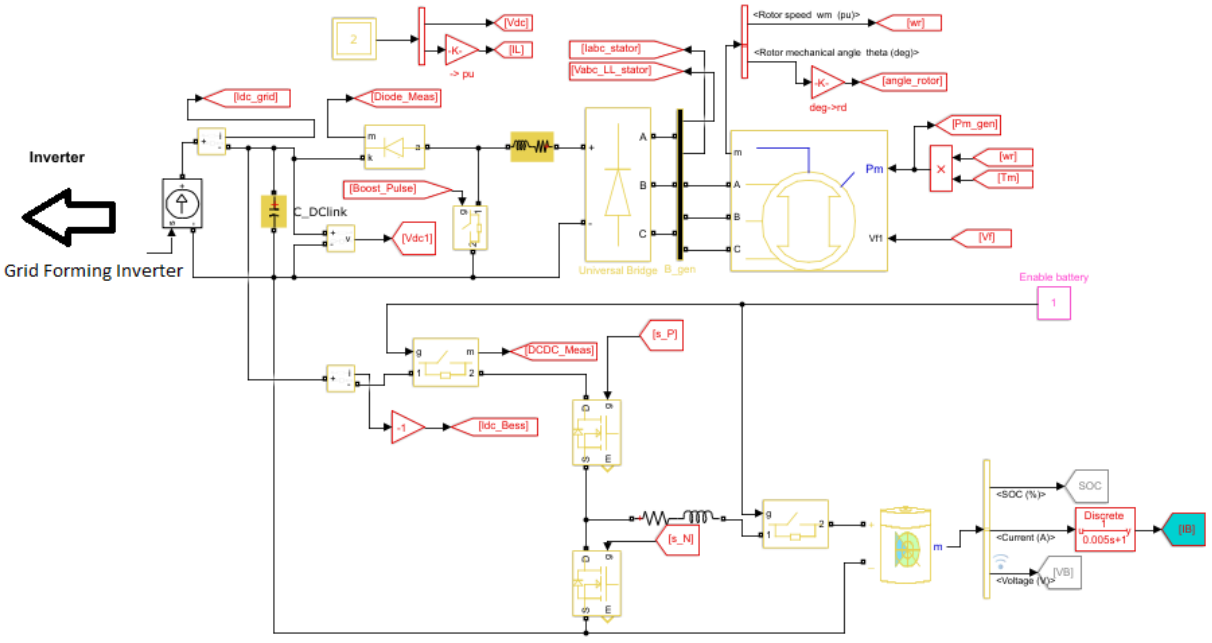

Figure 8. DC-coupled integrated BESS Simulink model

The integrated BESS helps smooth the variable power output of the wind turbine. The modeling details are found in (Poudel et al. 2021). The BESS can enhance the ability of the distributed wind turbine to provide various essential grid services described in Section 3 of this report, including black start operation.

This report is available at no cost from the National Renewable Energy Laboratory (NREL) at www.nrel.gov/publications.

2.4.5 Diesel Generator

The diesel generator is not permanently located at the Flatirons Campus but closely represents the generator used when the Flatirons Campus was operated as an island (Koralewicz Forthcoming). The diesel generator model for our simulation comprises three blocks (Figure 9): a synchronous machine, a diesel engine governor, and an excitation block. The nominal power of the synchronous machine is 2 MW, and line-to-line voltage is 460 V. The model of the diesel generator was tuned with step-response active and reactive power data from field measurements. The various parameters of the diesel generator model (the regulator gain) were tuned to match the measured data. This generator can maintain nominal system frequency and voltage of the microgrid in islanded operation.

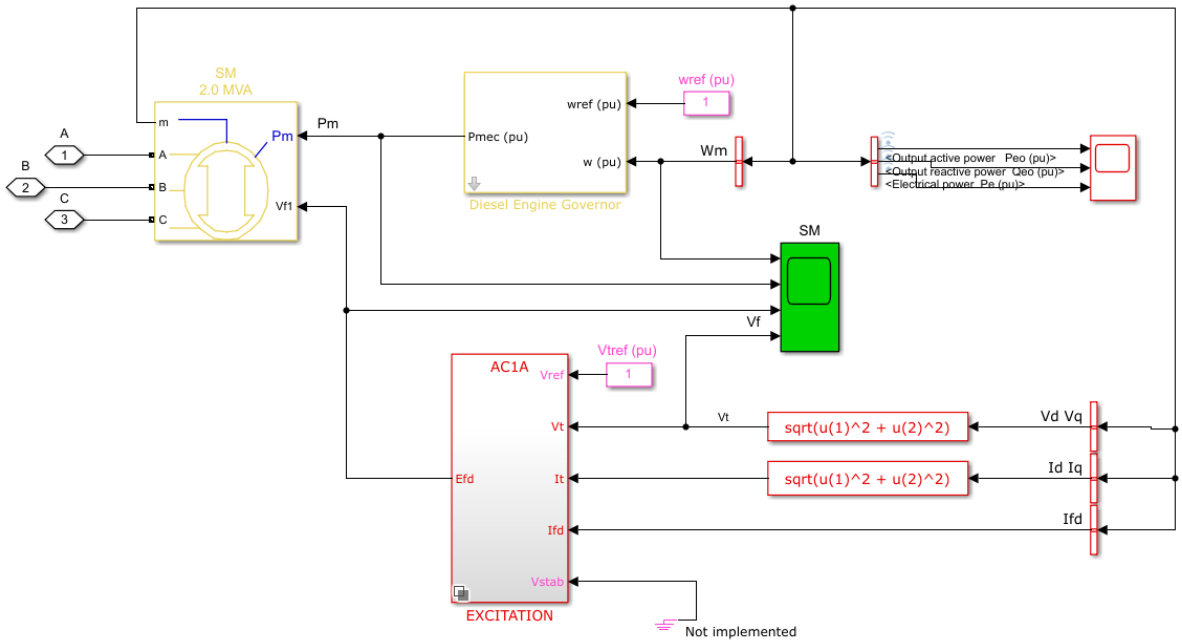

Figure 9. Simulink model of the 2-MW diesel generator

2.4.6 Loads

The microgrid model includes a critical load and a noncritical load. These load blocks are presented in Figure 10. Both blocks are fixed loads, but the critical load has more lenient trip thresholds than the noncritical load. This means that, in the event of a voltage or frequency instability, the noncritical load will trip first, which may stabilize the grid enough to prevent the critical load from tripping.

This report is available at no cost from the National Renewable Energy Laboratory (NREL) at www.nrel.gov/publications.

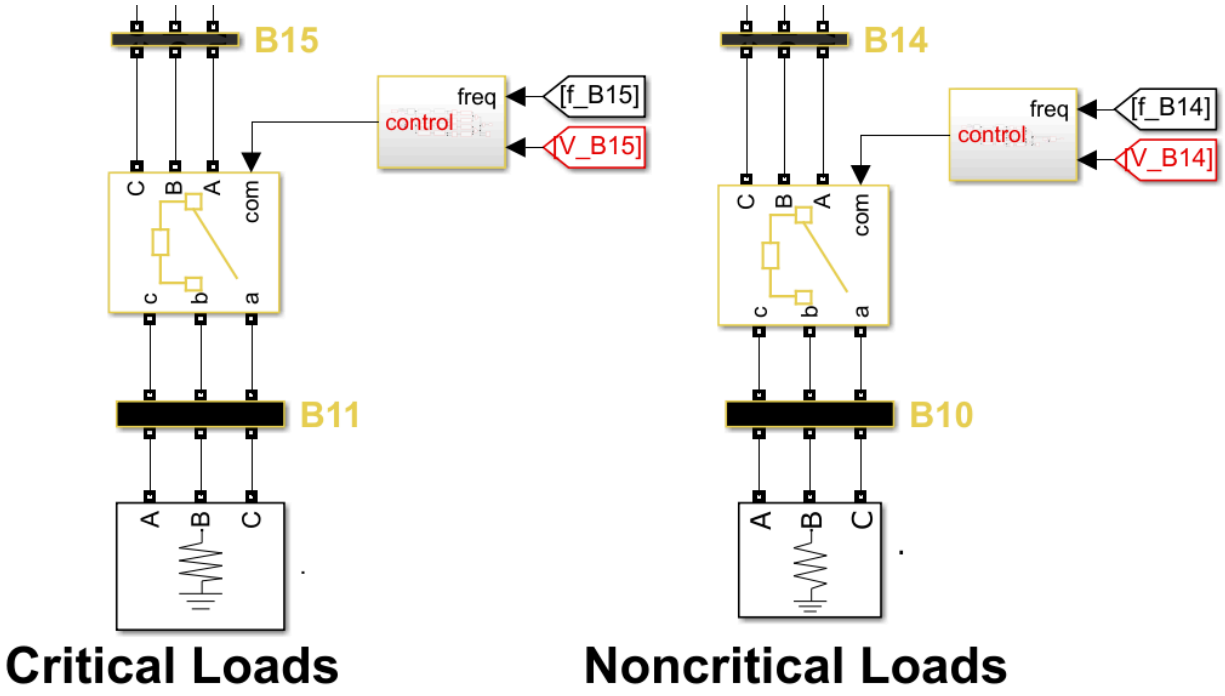

Figure 10. Critical and noncritical loads, with switches controlled by voltage and frequency stability

2.5 Transition and Dispatch

Transition and dispatch are important features of a microgrid connected to the utility grid (Institute of Electrical and Electronics Engineers [IEEE] 2017). Transition refers to connection to and disconnection from the utility grid using (in this model) a circuit breaker at the point of interconnection. The microgrid must be able to sustain its operation during transition in either direction. A transition from islanded mode to grid-connected mode requires synchronization, wherein the microgrid mirrors the characteristics of the utility grid (phase, frequency, and voltage) and supplies or absorbs the synchronized power. Dispatch refers to the connection of generating assets and storage to the microgrid. Transition and dispatch are control functions that present the microgrid as a single entity to the distribution grid.

Table 1, adapted from IEEE 2030.7-2017 (IEEE 2017), presents three levels of functions that are typical of a microgrid to satisfy interconnection requirements.

This report is available at no cost from the National Renewable Energy Laboratory (NREL) at www.nrel.gov/publications.

Table 1. Microgrid Control Functions and Levels

Microgrid Level	Microgrid Control Functions
Level 1: Lower-Level Functions (DER/Load)	• Voltage/frequency control • Real/reactive power control • Device-specific function.
Level 2: Core-Level Functions (Microgrid/Point of Interconnection)	• Transition (connect/disconnect) • Dispatch.
Level 3: Higher-Level Functions (Supervisory/distribution system operator)	• Operator interface • Optimal dispatch (grid/market) • Communication/supervisory control and data acquisition.

The two core-level functions (Level 2), which supervise the lower-level functions, are defined and specified in IEEE 2030.7-2017 as:

- The dispatch function dispatches individual devices in given operating modes with specified setpoints.
- The transition function supervises the transitions between connected and disconnected states, and ensures the dispatch is appropriate for the given state.

IEEE standard 1547-2018 (IEEE 2018a) supplies the parameters of synchronization as presented in Table 2.

Table 2. Synchronization Parameter Limits for the Grid Interconnection (Source: IEEE 2018a Table 5)

Aggregate Rating of DER Units (kilovolt-ampere [kVA])	Frequency Difference (Δf, hertz [Hz])	Voltage Difference (ΔV, %)	Phase Angle Difference ($\Delta\phi$, deg.)
0–500	0.3	10	20
>500–1,500	0.2	5	15
>1,500	0.1	3	10

We used $\Delta V = 10\%$, $\Delta f = 0.5$ Hz, and $\Delta\phi = 5°$ for the synchronization check. Upon complying with it, we operated the circuit breaker to connect and disconnect the utility grid. Connecting the diesel generator involves the same synchronization process. In the presence of abnormal voltage and frequency conditions, a microgrid may have to disconnect from the utility grid to ensure reliable operation of both.

This report is available at no cost from the National Renewable Energy Laboratory (NREL) at www.nrel.gov/publications.

3 Advanced Wind Turbine Controls

This section summarizes the advanced controls that enable distributed wind to provide essential grid services. Each function will be further investigated in follow-on reports specific to MIRACL use cases that employ the models described herein. The models also allow investigation of advanced wind control and integrated BESS that could open new opportunities for distributed wind turbine vendors to provide grid services.

Type III and Type IV wind turbines can regulate real and reactive power independently using a power electronics grid interface (NREL 2020). Wind turbines that are interfaced with power electronics can provide reactive power support even when they are not in operation or producing real power, such as when wind speed is below the cut-in speed. In this section, we describe the controls added to the CART averaged model to perform the desktop simulations of inertial response (North American Electric Reliability Corporation 2020), among others. The control modes developed include (1) inertial response, (2) primary frequency response, (3) real/reactive power control, (4) voltage response, and black start utilizing the grid-forming control. The user sets which mode the wind turbine will operate in. Primary frequency response and real power control define the real power command. Voltage response and reactive power control define the reactive power command, and inertial response defines the torque gain. All three are fed into the operational controller. Example simulations show the ability of the distributed wind turbine to provide inertial response, voltage response, and primary frequency response.

3.1.1 Inertial Response

Inertial response harvests rotor inertia to provide a temporary boost of power. The averaged model provides the option to use a frequency-based inertial controller or a torque-limited inertial controller (Wang et al. 2017, Muljadi et al. 2012). The torque-limited inertial controller is used in this report. This simple controller senses when frequency dips below a deadband around nominal frequency, and then commands maximum torque for 3 s to offset the dip. This action decelerates the rotor, extracting a portion of its kinetic energy and boosting the output power. After that, rotor inertia is recharged until the wind turbine returns to nominal speed, and then normal operation is resumed. Figure 11 displays the inertial response controller subsystem, which takes generator speed and grid frequency as inputs, and outputs torque command.

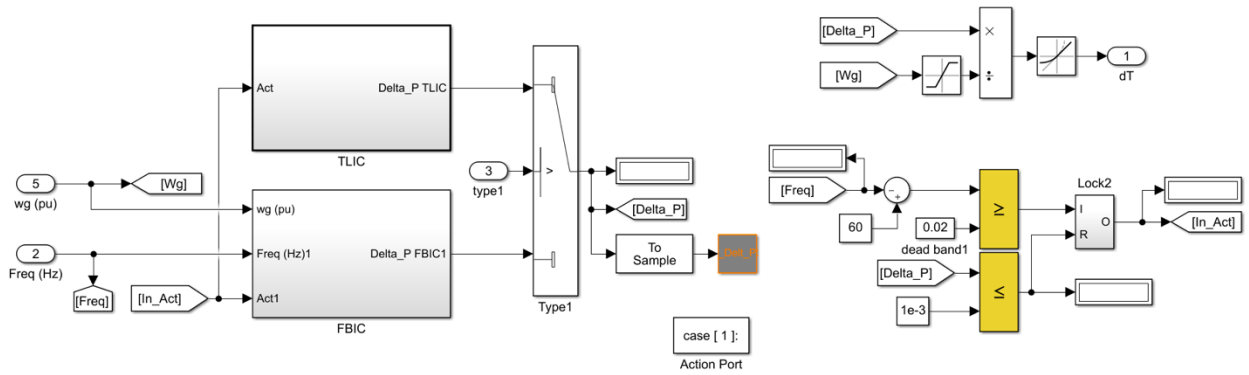

Figure 11. Inertial response controller subsystem with a torque-limited inertial controller (TLIC) and a frequency-based inertial controller (FBIC)

This report is available at no cost from the National Renewable Energy Laboratory (NREL) at www.nrel.gov/publications.

An example of inertial response is shown in Figure 12 for a stand-alone wind turbine. When frequency drops below a 0.02 Hz deadband, the torque-limited inertial controller is initiated, adding to the power command. This extra power is converted into a torque command (gain). When frequency dips at 10 s, torque gain ramps up to the limit of 1.3 per unit of the baseline value (pu), providing 3 s of extra power, which decelerates the rotor. Next, the torque and power dip as the rotor accelerates back to normal operating conditions. We note that the inertial response demonstrated in this model is weaker than that in wind turbine experiments. The mechanical torque has a slower than expected response to track the torque-gain signal, and the recovery is oscillatory instead of smooth. We postulate that the averaged model of the generator and power electronics or its operational controller prevent the modeled machine from providing inertial response as effectively as expected; future work will improve the averaged models and controls used in this illustration.

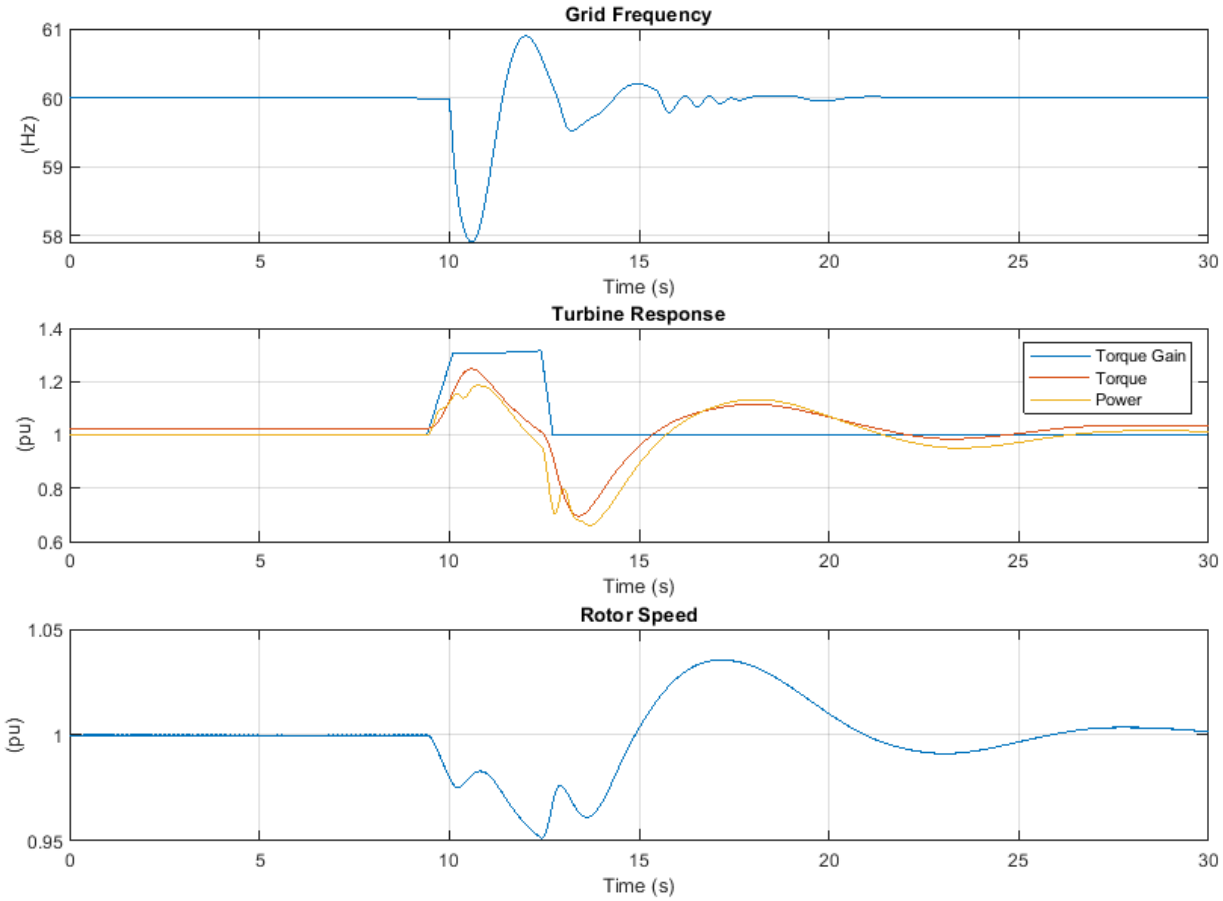

Figure 12. Torque-limited inertial controller response to a frequency dip

pu = per unit of the nominal value.

3.1.2 Primary Frequency Response

Primary frequency response starts with a wind turbine curtailed at around 0.9 pu at rated wind speed to provide headroom for supporting a frequency dip event by injecting available power. It is the only service that requires curtailment. When the frequency deviates above or below a 0.04% deadband, the power command responds opposite to the frequency deviation, with a 5%

This report is available at no cost from the National Renewable Energy Laboratory (NREL) at www.nrel.gov/publications.

droop (a 5% frequency change causes a 100% power command change in the opposite direction). Figure 13 displays the primary frequency response control as implemented in the Simulink model.

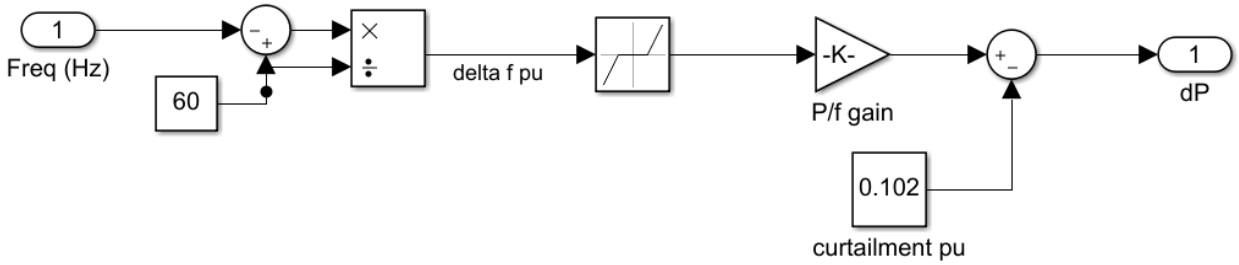

Figure 13. Primary frequency response droop controller subsystem

An example of the CART model performing primary frequency response is shown in Figure 14. Experimental data from a former NREL study (Ela et al. 2014) are used to validate the controls developed for this work. At 95 s, frequency drops below the deadband, and the power command increases to counteract the frequency drop. Power output lags the command by less than 5 s throughout the response. The power output from the simulation matches the experimental data well, except for an initial undershoot of the curtailment command at 20 s when curtailment begins. We postulate that this is an artifact of the averaged model, which can be further improved through tuning or by using a detailed model.

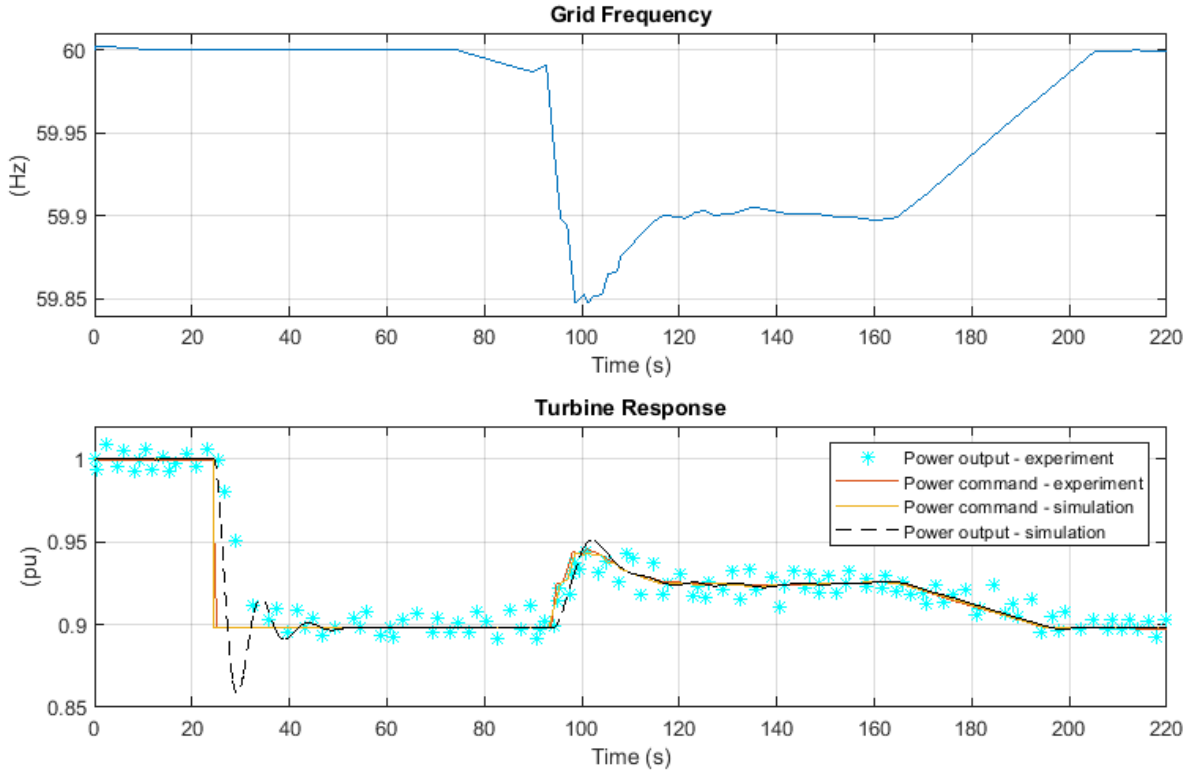

Figure 14. Primary frequency response to a frequency dip. Simulated results follow the experimental results well, except at the initial curtailment where there are some oscillations, which we are still working to resolve in the model.

This report is available at no cost from the National Renewable Energy Laboratory (NREL) at www.nrel.gov/publications.

3.1.3 Voltage Response

Voltage response is like primary frequency response, except it responds to a deviation in voltage with an increase in the reactive power command. In this model, 10% droop is used. The amount of reactive power injected also depends on the allowed control set points for maximum reactive power. Figure A.1 displays the voltage response control subsystem. An example of the CART performing voltage response, compared to its baseline case (producing maximum power with no voltage response), is shown in Figure 15. When the bus voltage drops below its nominal value due to a fault at 10 s, the reactive power command increases to elevate the voltage, increasing the voltage nadir and reducing response time relative to the baseline case.

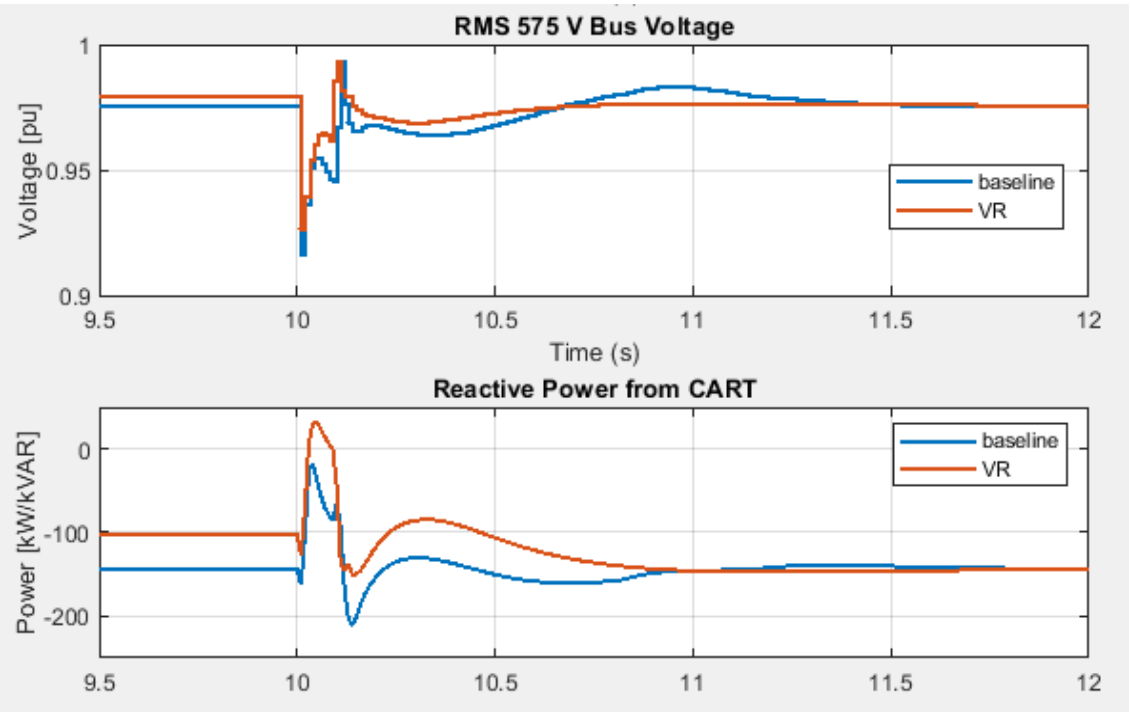

Figure 15. Reactive power support from wind turbine.

Baseline = wind turbine provides no voltage response. VR = wind turbine provides voltage response.

3.1.4 Real and Reactive Power Command Tracking

In real/reactive power control mode, real and reactive power commands are fed directly into the model instead of being calculated by a voltage or frequency deviation. Figure 16 displays the CART responding to such commands. This logic can also be used to track a power factor.

This report is available at no cost from the National Renewable Energy Laboratory (NREL) at www.nrel.gov/publications.

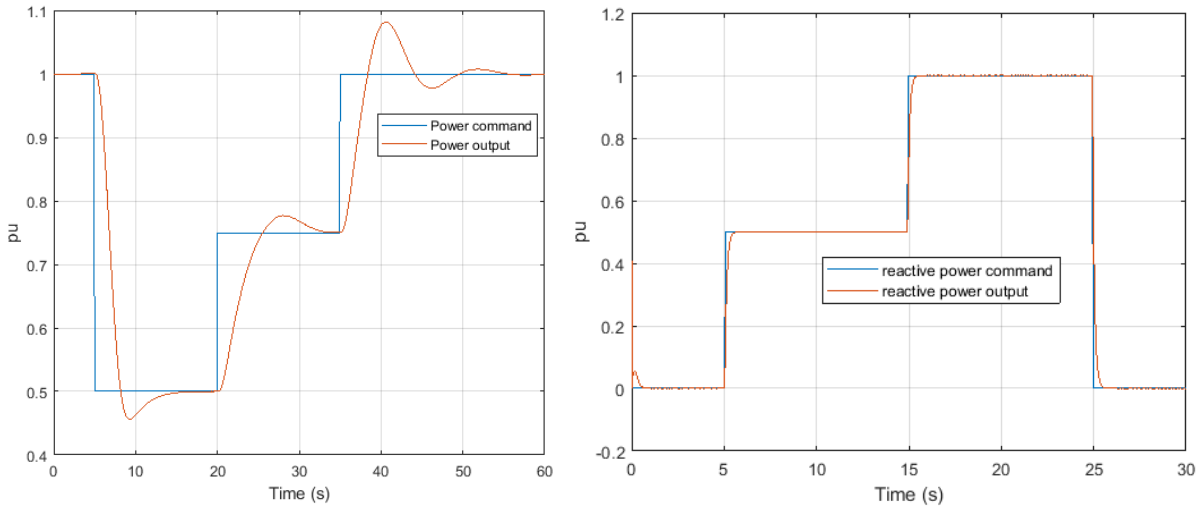

(a) (b)

Figure 16. Wind turbine following (a) real and (b) reactive power command

3.1.5 Wind Turbine Hybrid Model Controls for Voltage Faults

The relevant control logic of the grid-side inverter model, used for its superior reactive power performance, is explained in this section at a high level. More details are found in the Appendix.

In most situations, reactive current is calculated with a proportional-integral controller that tracks a given reactive power reference. This reference can be commanded directly for either reactive power tracking or power factor tracking. Real current is calculated with a proportional-integral controller that tracks a given nominal DC-link voltage. This tracking stabilizes power output during voltage faults.

During a mild voltage fault, the wind turbine provides a reactive power response via droop control, as displayed in Figure 1. The control system injects reactive power for undervoltage and absorbs reactive power for overvoltage to stabilize the grid voltage. Normally, real current is prioritized. However, in this situation, reactive current is prioritized to enable the desired response.

During a moderate voltage fault, the wind turbine rides through before tripping after a specified amount of time. It does not provide a significant power response.

During a severe voltage fault, the wind turbine performs “momentary cessation”: the proportional-integral controllers are overridden, and real and reactive currents are controlled directly. Real current is zeroed during the fault and then ramped up to its nominal value when voltage recovers. Reactive current is slightly elevated during the fault, and then ramped down to its nominal value when the fault ends, at which point proportional-integral control is resumed. The real and reactive power response times are set by controller inputs. If voltage does not recover, the wind turbine trips. All three functionalities are demonstrated in the grid-connected use case.

This report is available at no cost from the National Renewable Energy Laboratory (NREL) at www.nrel.gov/publications.

3.1.6 Real-World Implementation

Typical control structures for microgrids or hybrid systems are hierarchical (Bidram and Davoudi 2012) with (1) local, device-level control (for example, wind turbine, solar PV array, diesel generator, or BESS) for device protection, ride-through, and grid support in response to local measurements; (2) plant-level control, in which coordination with a central dispatcher is desired; and (3) tertiary control that manages interactions with the grid.

In a real-world system, modifications to both the device-level and plant-level controls would be necessary to implement the advanced controls demonstrated here. At the device level, modifications to each control program would be implemented in a similar fashion to this report. The details of the implementation would depend on the specific controller of the wind turbine or DER in question. This report demonstrates simple logic that enables these functionalities; however, implementation on real machines may be more complex. At the plant level, the controller would need to be incorporated either with existing controls or as a peripheral control, which may require the original equipment manufacturer to unlock some channels. A tertiary-level controller will be implemented in future work. If included in a real system, it would select which control modes would run the wind turbine and DERs at any given time, and it would contain logic to determine how each control mode would interact with its regular dispatch logic.

A wind turbine can control real and reactive power by various means such as rotor speed control, rotor pitch control, yaw control, and inverter control. Because the CART is a Type IV machine, we focus on the control of the inverter through power electronics-based vector current control. The amount of real or reactive power modulation depends on the size of the grid-side inverter and whether real or reactive power is prioritized.

To provide grid services, a wind turbine receives various sensor and command inputs, which it feeds into its control system, which then commands certain outputs. Table 3 describes the inputs, control parameters, and outputs corresponding to each service. This information reflects the Type IV wind turbine averaged model used in this report, and because the information will vary based on wind turbine architecture, it should be considered an example. In the CART model, sensor or command inputs determine certain control parameters: real power reference, reactive power reference, and boost converter current reference (corresponding to torque reference). The references are fed into the pitch controller, reactive current controller, and boost converter (which functionally commands generator electrical torque). These commands affect the real and reactive power output of the wind turbine.

There are two main configurations in which a distributed wind turbine would provide essential grid services. First, a stand-alone wind turbine can provide inertial response, primary frequency response, and voltage response by controlling the inverters utilizing some of the advanced controls mentioned in this section. Second, the wind turbine can work in synergy with a BESS (either AC- or DC-coupled) to provide the required flexibility and reliability services (Poudel et al. 2021; Das et al. 2019), including black start. The black start feature may demand extra investment, as it may require a sequential start-up operation by a grid-forming inverter and the battery storage.

This report is available at no cost from the National Renewable Energy Laboratory (NREL) at www.nrel.gov/publications.

Table 3. Inputs, Control Parameters, and Outputs for Each Grid Service

Grid Service	Input Sensor/Command	Control Parameter	Output
Inertial Response	Grid Frequency	Boost Converter Current Reference	Real Power
Primary Frequency Response	Grid Frequency	Real Power Reference	Real Power
Voltage response	Grid Voltage	Reactive Power Reference	Reactive Power
Real Power Control	Real Power Command	Real Power Reference	Real Rower
Reactive Power Control	Reactive Power Command	Reactive Power Reference	Reactive Power
Power Factor Control	Power Factor Command	Reactive Power Reference	Reactive Power

This report is available at no cost from the National Renewable Energy Laboratory (NREL) at www.nrel.gov/publications.

4 Conclusion

The MIRACL project used MATLAB Simulink to model a small portion of NREL's Flatirons Campus assets to demonstrate how the advanced control capabilities of distributed wind turbines can benefit the grid in various use cases. Models of the wind turbine, solar PV plant, diesel generator, BESS, inverters, and loads comprising this microgrid were developed using MATLAB Simulink. Advanced controls enabled various functionalities to be incorporated into the models to comply with the grid code and with standards such as IEEE 1547-2018 and IEEE 2030.7-2017.

This report is the first in a series of four that review the models developed under MIRACL. The models and underlying functionalities serve as an introduction to the following reports that detail the four MIRACL use cases. Part 2 of this series covers wind turbines in isolated grids, Part 3 covers the grid-connected distributed wind turbine deployments (both behind the meter and in front of the meter), and Part 4 covers wind turbines in microgrids, including island and grid-connected operation, as well as transitions and dispatch.

This report is available at no cost from the National Renewable Energy Laboratory (NREL) at www.nrel.gov/publications.

References

Anderson, Ben. 2021. *Flatiron-Campus-Microgrid.* MATLAB. https://github.com/badeshiben/Flatiron-Campus-Microgrid.

Ashuri, Turaj, Mario A. Rotea, Yan Xiao, Yaoyu Li, and Chandra V. Ponnurangam. 2016. "Wind Turbine Performance Decline and Its Mitigation via Extremum Seeking Controls." Presented at American Institute of Aeronautics and Astronautics AIAA SciTech, 34th Wind Energy Symposium, San Diego, CA, Jan. 4–8, 2016.

Bidram, Ali, and Ali Davoudi. 2012. "Hierarchical Structure of Microgrids Control System." *IEEE Transactions on Smart Grid* 3(4): 1963–1976. https://doi.org/10.1109/TSG.2012.2197425.

Das, Kaushik, Anca D. Hansen, Panagiota Adamou, Xenofon Giagkou, Filippos Rigas, Jayachandra Sakamuri, and Poul E Sørensen, Mufit Altin, and Edgar Nuno. 2019. "Dynamic Modelling of Wind Solar Storage Based Hybrid Power Plant." Presented at the 18th Wind Integration Workshop, Dublin, Ireland, Oct. 16–18, 2019.

Ela, E., V. Gevorgian, P. Fleming, Y. C. Zhang, M. Singh, E. Muljadi, A. Scholbrook, et al. 2014. *Active Power Controls From Wind Power: Bridging the Gaps.* Golden, CO: National Renewable Energy Laboratory. NREL/TP-5D00-60574. https://www.nrel.gov/docs/fy14osti/60574.pdf.

Fingersh, L. J., and K. Johnson. 2002. *Controls Advanced Research Turbine (CART) Commissioning and Baseline Data Collection.* Golden, CO: National Renewable Energy Laboratory. NREL/TP-500-32879. https://www.nrel.gov/docs/fy03osti/32879.pdf.

Gagnon, Richard, and Jacques Brochu. 2020. "Wind Farm - Synchronous Generator and Full Scale Converter (Type 4) Detailed Model." MathWorks, Inc. Accessed September 15, 2020. https://www.mathworks.com/help/physmod/sps/ug/wind-farm-synchronous-generator-and-full-scale-converter-type-4-detailed-model.html.

Institute of Electrical and Electronics Engineers (IEEE). 2017. *Standard for the Specification of Microgrid Controllers*. IEEE 2030.7-2017. IEEE. https://doi.org/10.1109/IEEESTD.2018.8340204.

IEEE. 2018a. *Standard for Interconnection and Interoperability of Distributed Energy Resources with Associated Electric Power Systems Interfaces*. IEEE 1547-2018. IEEE. https://standards.ieee.org/ieee/1547/5915/.

IEEE. 2018b. *IEEE Standard for Interconnection and Interoperability of Distributed Energy Resources With Associated Electric Power Systems Interfaces*. IEEE 1547-2018. IEEE. https://standards.ieee.org/ieee/1547/5915/.

Koralewicz, Przemyslaw, Robert Wallen, and Emanuel Mendiola. Forthcoming. "Unleashing the Frequency—Multimegawatt Demonstration of 100% Renewable Power Systems with Decentralized Communication-Less Control Scheme." Golden, CO: National Renewable Energy Laboratory. NREL/TP-5000-80742.

This report is available at no cost from the National Renewable Energy Laboratory (NREL) at www.nrel.gov/publications.

Kuga, Roy, Mark Esguerra, Bennett Chabot, and Alejandro Avendaño Ceceña. 2019. "Pacific Gas and Electric Company EPIC Final Report." https://www.pge.com/pge_global/common/pdfs/about-pge/environment/what-we-are-doing/electric-program-investment-charge/PGE-EPIC-Project-2.05.pdf.

MathWorks. 2020. "250-kW Grid-Connected PV Array." https://www.mathworks.com/help/physmod/sps/ug/250-kw-grid-connected-pv-array.html.

Muljadi, Eduard, Vahan Gevorgian, Mohit Singh, and Surya Santoso. 2012. *Understanding Inertial and Frequency Response of Wind Power Plants: Preprint*. Golden, CO: National Renewable Energy Laboratory. NREL/CP-5500-55335. https://www.nrel.gov/docs/fy12osti/55335.pdf.

National Renewable Energy Laboratory. n.d. "Flatirons Campus Research Laboratories & Facilities." https://www.nrel.gov/wind/assets/pdfs/wind-capabilites-laboratories-and-facilities.pdf.

National Renewable Energy Laboratory. 2020. "Power Electronic Grid Interface Platform Workshop." https://www.nrel.gov/aries/power-electronic-grid-interface-workshop.html.

North American Electric Reliability Corporation. 2020. *Fast Frequency Response Concepts and Bulk Power System Reliability Needs.* Atlanta, GA (United States): North American Electric Reliablity Corporation. https://www.nerc.com/comm/PC/InverterBased%20Resource%20Performance%20Task%20Force%20IRPT/Fast_Frequency_Response_Concepts_and_BPS_Reliability_Needs_White_Paper.pdf.

Poudel, Ram, Venkat Krishnan, James Reilly, Przemyslaw Koralewicz, and Ian Baring-Gould. 2021. *Integration of Storage in the DC Link of a Full Converter-Based Distributed Wind Turbine: Preprint*. Golden, CO: National Renewable Energy Laboratory. NREL/CP-5000-78347. https://www.nrel.gov/docs/fy21osti/78347.pdf.

Reilly, Jim, Jake Gentle, Alice Orrell, and Brian Naughton. 2021. *Microgrids, Infrastructure Resilience, and Advanced Controls Launchpad (MIRACL): Use Cases and Definitions.* Golden, CO: National Renewable Energy Laboratory. NREL/TP-7A40-76918. https://www.nrel.gov/docs/fy21osti/76918.pdf.

Reilly, Jim, Ram Poudel, Venkat Krishnan, Robert Preus, Ian Baring-Gould, Ben Anderson, Brian Naughton, Felipe Wilches-Bernal, and Rachid Darbali. 2021. *Distributed Wind Controls: A Research Roadmap for Microgrids, Infrastructure Resilience, and Advanced Controls Launchpad (MIRACL)*. Golden, CO: National Renewable Energy Laboratory. NREL/TP-7A40-76748. https://www.nrel.gov/docs/fy21osti/76748.pdf.

Trevisan, Aramis Schwanka, Amgad A. El-Deib, Richard Gagnon, Jean Mahseredjian, and Martin Fecteau. 2018. "Field Validated Generic EMT-Type Model of a Full Converter Wind Turbine Based on a Gearless Externally Excited Synchronous Generator." *IEEE Transctions on Power Delivery* 33(5): 2284–2293. https://doi.org/10.1109/TPWRD.2018.2850848.

This report is available at no cost from the National Renewable Energy Laboratory (NREL) at www.nrel.gov/publications.

Trevisan, Aramis Schwanka. 2019. *Generic Type-IV Wind Turbine Model.* MATLAB Central File Exchange. https://www.mathworks.com/matlabcentral/fileexchange/71235-type-iv-wind-turbine.

Wang, Xiao, David Wenzhong Gao, Jianhui Wang, Weihang Yan, Wei Gao, Eduard Muljadi, and Vahan Gevorgian. 2018. "Implementations and Evaluations of Wind Turbine Inertial Controls With FAST and Digital Real-Time Simulations." *IEEE Transactions on Energy Conversion* 33(4): 1805–1814. https://doi.org/10.1109/TEC.2018.2849022.

Wang, Xiao, Wenzhong Gao, Weihang Yan, Jianhui Wang, Eduard Muljadi, Vahan Gevorgian and Andrew Scholbrock. 2017. "Evaluation of the Inertial Response of Variable-Speed Wind Turbines Using Advanced Simulation." *IEEE Power & Energy Society General Meeting.* Chicago, IL, July 16–20, 2017. https://doi.org/10.1109/PESGM.2017.8274390.

This report is available at no cost from the National Renewable Energy Laboratory (NREL) at www.nrel.gov/publications.

Appendix

To model reactive power controls, we use grid-side inverter controls adapted from a wind turbine model developed by Trevisan et al. (2018). The model is a hybrid type that provides accuracy near that of a detailed model with the computational time of an averaged model. The relevant voltage fault ride-through (FRT) logic is explained in this section.

The wind turbine has two voltage FRT modes. In the first mode, FRT1, the wind turbine injects or absorbs reactive power to counteract a voltage dip or rise, respectively. FRT 1 is voltage-reactive power mode, as defined in IEEE 1547 (IEEE 2018b). In the second mode, FRT2, the wind turbine provides no real power and elevated reactive power to the grid during a fault, and ramps real power back up and reactive power back down after the voltage recovers. FRT 2 is momentary cessation, as defined in IEEE 1547 (IEEE 2018b).

The response of both the model and a physical machine equipped with FRT to voltage faults is dependent on the FRT mode that is selected. Grid voltage at the point of connection is an input into the control logic, which controls the real and reactive current references fed into the grid-side inverter. This inverter outputs real and reactive power based on these references.

In most situations, reactive current is calculated with a proportional-integral controller that tracks a given reactive power reference, and real current is calculated with a proportional-integral controller that tracks a given nominal DC-link voltage. This tracking stabilizes power output during voltage faults. In FRT1, when voltage exits the deadband but remains in the continuous operation zone, the wind turbine provides a reactive power response via droop control. The control system injects reactive power for undervoltage and absorbing reactive power for overvoltage to stabilize the grid voltage. The magnitude of active power is given by the following equations (IEEE 2018b):

Operation for low-frequency conditions:

$$p = \min_{f<60-db_{UF}} \left\{ p_{pre} + \frac{(60 - db_{UF}) - f}{60 \cdot k_{UF}} ; p_{avl} \right\} \quad \text{(A.1)}$$

Operation for high-frequency conditions:

$$p = \max_{f>60+db_{OF}} \left\{ p_{pre} + \frac{f - (60 + db_{OF})}{60 \cdot k_{OF}} ; p_{min} \right\} \quad \text{(A.2)}$$

where

p = the real power output, in pu, of the nameplate real power rating
f = the disturbed system frequency, in hertz (Hz)
p_{avl} = the available real power, in pu
p_{pre} = the predisturbance real power output, defined by the active power output at the point of time the frequency exceeds the deadband, in pu

This report is available at no cost from the National Renewable Energy Laboratory (NREL) at www.nrel.gov/publications.

p_{min} = the minimum real power output, in pu
db_{OF} = a single-sided deadband value for high frequency, in Hz
db_{UF} = a single-sided deadband value for low frequency, in Hz
$k_{OF/UF}$ = the pu frequency changes corresponding to 1 pu power output change (droop).

Normally, real current is prioritized. However, in this situation, reactive current is prioritized to enable the desired response. The nonprioritized current is limited according to:

$$i_{\mathrm{dlim}}^2 = i_{\mathrm{max}}^2 - i_{\mathrm{qlim}}^2 \tag{A.3}$$

where

i_{dlim} = the real current limit, in amperes (A)
i_{qlim} = the reactive current limit, in A
i_{max} = the maximum current allowed in the system, in A.

In FRT2, when the voltage enters the momentary cessation zones, the proportional-integral controllers are overridden, and real and reactive currents are controlled directly. Real current is zeroed during the fault, and then ramped up to its nominal value when the fault ends. Reactive current is slightly elevated during the fault, and then ramped down to its nominal value when the fault ends, at which point proportional-integral control is resumed. The real and reactive power response times are set by controller inputs.

In either mode, the wind turbine rides through faults in the mandatory operation zone, tripping after a specified amount of time. A detailed implementation in terms of the Simulink block diagram is available in (Trevisan et al. 2018), and we attempt to explain some relevant sections of the model in the following three figures.

Figure A.1 shows the voltage/reactive current droop control in FRT1. This logic determines the reactive current for the FRT (iq_FRT). This logic determines if the system is in undervoltage (UVRT) or overvoltage (OVRT) condition by comparing it with their respective thresholds (V_uvrt for undervoltage and V_ovrt for overvoltage) with the grid voltage at point of common coupling (Vpcc). In an undervoltage condition, the value of Vpcc is below the undervoltage threshold (Vpcc < V_uvrt), and in an overvoltage condition, the value of Vpcc is above the overvoltage threshold (Vpcc > V_ovrt). If either case is true, it triggers the appropriate UVRT or OVRT binary signal. k_uvrt and k_ovrt are the respective droop gains, and i_rated is the rated current gain, which is applied to the difference in the measured Vpcc value and the threshold to determine the appropriate reactive current response (iq_FRT) to ride through the fault condition.

This report is available at no cost from the National Renewable Energy Laboratory (NREL) at www.nrel.gov/publications.

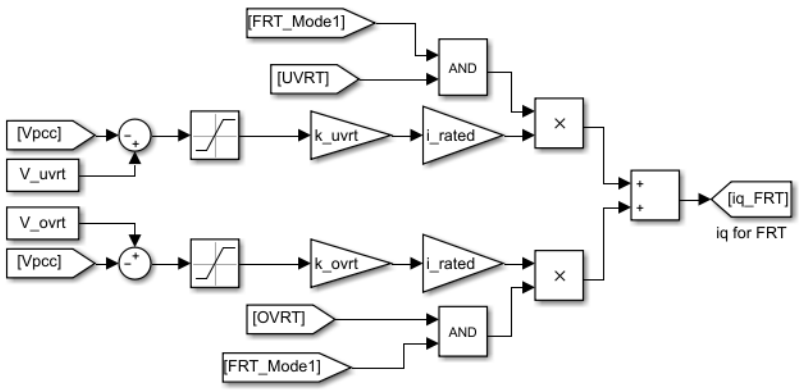

Figure A.1. Voltage/reactive current droop control

Figure A.2 displays real and reactive current limit calculations. i_max is maximum current, i_q is reactive current reference, i_d is real current reference, reac_prio is a binary signal (which is 1/0 if reactive/real power is prioritized), i_d_lim is real current limit, and i_q_lim is reactive current limit. The limits are dynamically adjusted based on whether real or reactive power are prioritized. Real power is prioritized if not in FRT, and reactive power is prioritized if in FRT. id(iq)0_FRT2 is the real(reactive) current specified for FRT2, and reset_id(iq)_FRT is a binary signal, which is 1 during a fault if FRT2 is selected. When a fault occurs, real current is zeroed during the fault and ramps back up after the voltage recovers. Reactive current is slightly elevated during the fault and ramps back down afterward.

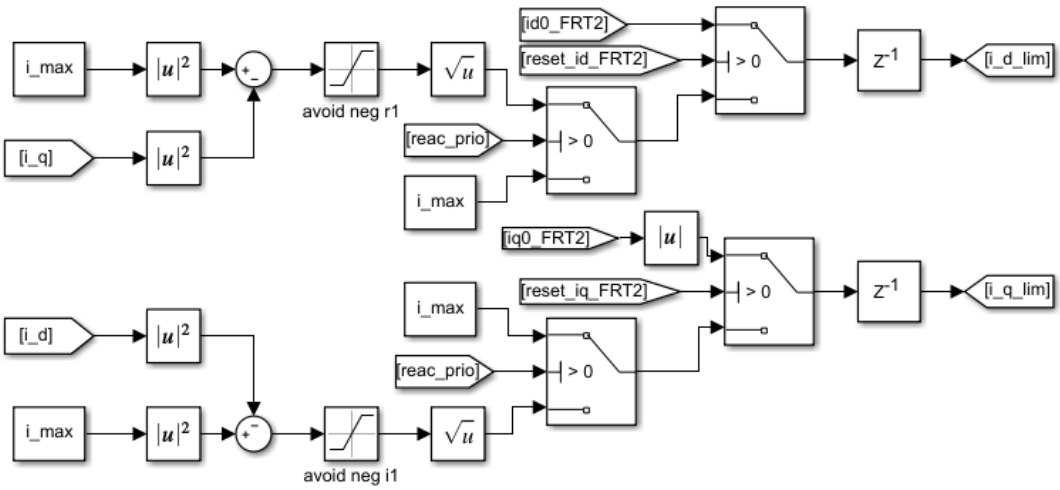

Figure A.2. Real and reactive power priority implementation

The real current is based on the DC voltage and reactive current is based on the reactive power deviation.

Figure A.3 displays proportional-integral controllers used to calculate the real and reactive current references. Protection is a binary signal, which is 1 if the wind turbine is connected to the grid, and FRT_Mode is a flag, which is 1/2 if FRT1/2 is selected. Vdc_filt is the filtered DC voltage, Vdc_ref is the DC voltage reference, Q_ref_filt is the filtered reactive power reference, Q_meas_filt is the filtered measured reactive power, and FRT_flag is a binary signal, which is 1

This report is available at no cost from the National Renewable Energy Laboratory (NREL) at www.nrel.gov/publications.

if in FRT. Real current is limited by i_d_lim calculated in Figure A.2. In FRT1, when FRT is no longer active (e.g., when voltage recovers), i_d is reset to the value immediately prior to FRT being activated. In FRT2, if a fault occurs, i_d is directly controlled by id0_FRT2, as in Figure A.2.

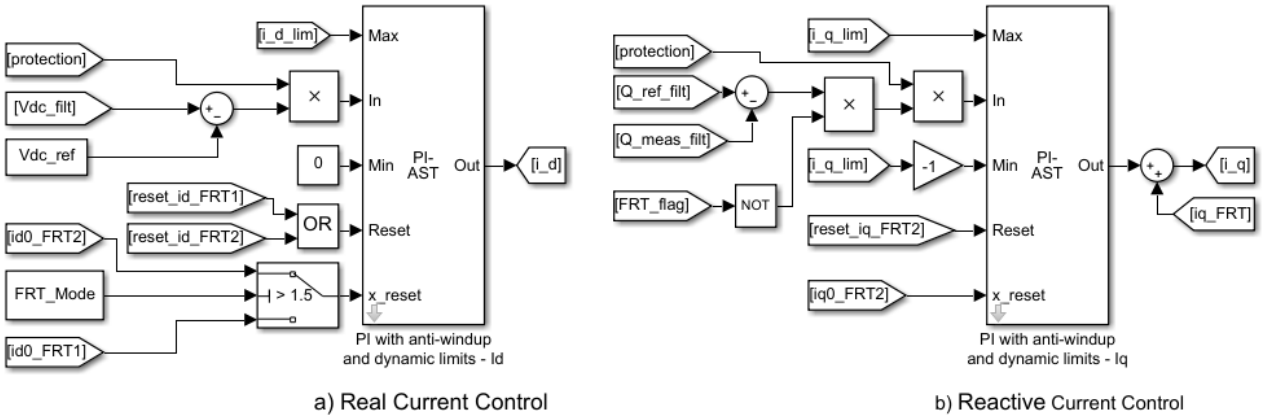

Figure A.3. Proportional-integral controllers for (a) real (Id) and (b) reactive (Iq) currents

If not in FRT, reactive current is calculated from the reactive power deviation. In the case of FRT1, i_q = iq_FRT, calculated by the droop control in Figure A.1. If in FRT2, reactive current is directly controlled by the iq0_FRT2 signal, as presented in Figure A.2.

Figure A.4 presents the response of the wind turbine for an isolated voltage event for two values of k_UVRT (Trevisan 2019). The voltage dip at 1 s is below the undervoltage trigger value (0.8 pu); hence, there is a response by the wind turbine in terms of real power and reactive power. The P and Q ramp time depends on these gains and other parameters presented above.

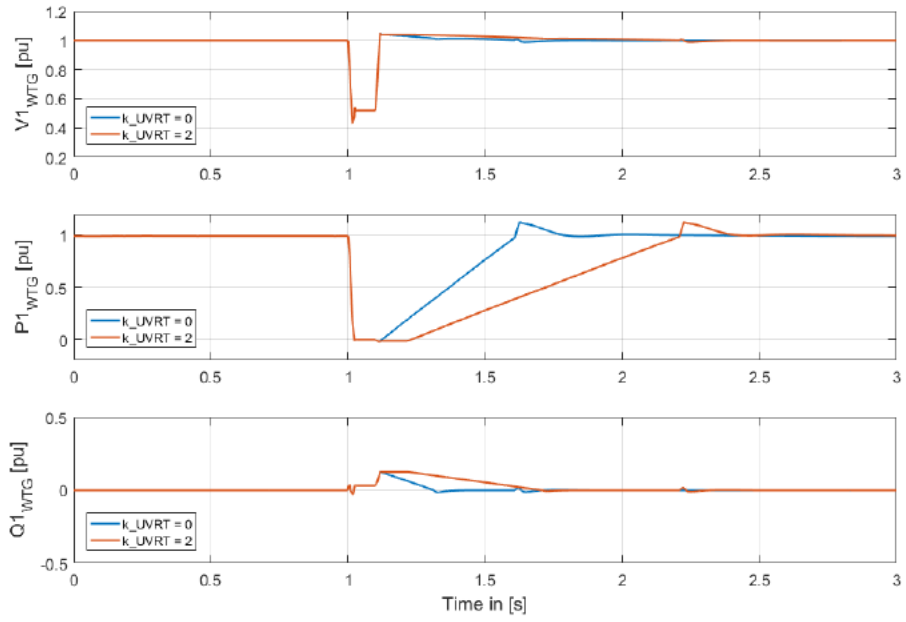

Figure A.4. Effect of parameters on real and reactive power response of the wind turbine.

$Q1_{WTG}$ = reactive power; $P1_{WTG}$ = real power; $V1_{WTG}$ = voltage; k_UVRT = undervoltage ride-through.

This report is available at no cost from the National Renewable Energy Laboratory (NREL) at www.nrel.gov/publications.